



OPEN

Cathepsin S provokes interleukin-6 (IL-6) trans-signaling through cleavage of the IL-6 receptor in vitro

Charlotte M. Flynn¹, Yvonne Garbers², Stefan Düsterhöft³, Rielana Wichert¹, Juliane Lokau⁴, Christian H. K. Lehmann^{5,6}, Diana Dudziak^{5,6}, Bernd Schröder⁷, Christoph Becker-Pauly¹, Stefan Rose-John¹, Samadhi Aparicio-Siegmund¹ & Christoph Garbers⁴✉

The cytokine interleukin-6 (IL-6) fulfills its pleiotropic functions via different modes of signaling. Regenerative and anti-inflammatory activities are mediated via classic signaling, in which IL-6 binds to the membrane-bound IL-6 receptor (IL-6R). For IL-6 trans-signaling, which accounts for the pro-inflammatory properties of the cytokine, IL-6 activates its target cells via soluble forms of the IL-6R (sIL-6R). We have previously shown that the majority of sIL-6R in human serum originates from proteolytic cleavage and mapped the cleavage site of the IL-6R. The cleavage occurs between Pro-355 and Val-356, which is the same cleavage site that the metalloprotease ADAM17 uses in vitro. However, sIL-6R serum levels are unchanged in hypomorphic ADAM17^{ex/ex} mice, making the involvement of ADAM17 questionable. In order to identify other proteases that could be relevant for sIL-6R generation in vivo, we perform a screening approach based on the known cleavage site. We identify several candidate proteases and characterize the cysteine protease cathepsin S (CTSS) in detail. We show that CTSS is able to cleave the IL-6R in vitro and that the released sIL-6R is biologically active and can induce IL-6 trans-signaling. However, CTSS does not use the Pro-355/Val-356 cleavage site, and sIL-6R serum levels are not altered in *Ctss*^{-/-} mice. In conclusion, we identify a novel protease of the IL-6R that can induce IL-6 trans-signaling, but does not contribute to steady-state sIL-6R serum levels.

Interleukin-6 (IL-6) is the founding and name-giving member of the IL-6 family of cytokines¹. In healthy humans, IL-6 serum levels are in the low pg/ml range or even undetectable. However, during inflammatory events, IL-6 levels rise dramatically and can even reach amounts of several µg/ml in patients with sepsis². The involvement of IL-6 in practically all human inflammatory diseases has made the cytokine an important therapeutic target, and antibodies targeting either IL-6 or the IL-6 receptor (IL-6R) are used in the clinics, e.g. for the treatment of rheumatoid arthritis, cytokine release syndrome and Castleman disease^{3,4}.

IL-6 activates its target cells by binding to the IL-6 receptor (IL-6R), which is mainly expressed on hepatocytes and different leukocyte subsets like T cells, B cells, megakaryocytes and neutrophils⁵. The formation of the IL-6/IL-6R complex induces homodimerization of the common β-receptor glycoprotein (gp)130 and subsequently the activation of several intracellular signaling cascades, e.g. the Janus kinase/Signal Transducer and Activator of Transcription (Jak/STAT), the phosphoinositide 3-kinase (PI3K) and the mitogen-activated protein kinase (MAPK) pathways⁶. This mode of signaling has been termed classic signaling and is thought to be responsible for the regenerative, anti-inflammatory properties of IL-6^{3,7}.

¹Institute of Biochemistry, Kiel University, Kiel, Germany. ²Institute of Psychology, Kiel University, Kiel, Germany. ³Institute of Molecular Pharmacology, RWTH Aachen University, Aachen, Germany. ⁴Department of Pathology, Medical Faculty, Otto-Von-Guericke-University Magdeburg, Magdeburg, Germany. ⁵Laboratory of Dendritic Cell Biology, Department of Dermatology, University Hospital Erlangen, Friedrich-Alexander University of Erlangen-Nürnberg, Erlangen, Germany. ⁶Deutsches Zentrum Immuntherapie (DZI) and Medical Immunology Campus Erlangen, Erlangen, Germany. ⁷Institute for Physiological Chemistry, Medizinisch-Theoretisches Zentrum MTZ, Technische Universität Dresden, Fiedlerstraße 42, 01307 Dresden, Germany. ✉email: christoph.garbers@med.ovgu.de

Besides classic signaling, IL-6 can also bind to and signal via soluble variants of the IL-6R (sIL-6R). The resulting IL-6/sIL-6R complex activates cells via gp130 homodimerization in an agonistic manner and by this mechanism significantly expands the number of cell types that can be activated by IL-6, as gp130 is expressed ubiquitously and IL-6 does not require membrane-bound IL-6R expression. This so-called trans-signaling is responsible for the pro-inflammatory actions of the cytokine^{8,9}. In healthy humans, sIL-6R serum levels are in the range of 20–80 ng/ml¹⁰. A single nucleotide polymorphism (rs2228145), which results in the exchange of an asparagine into an alanine residue at position 358 of the IL-6R protein in close proximity of the ADAM17 cleavage site, results in increased sIL-6R levels^{11,12} and is associated with a reduced risk of coronary heart disease^{13,14}. The reason for this might be an anti-inflammatory effect on an increased buffer capacity of sIL-6R in combination with soluble gp130 (sgp130), which can bind and thus neutralize low levels of systemic IL-6^{15,16}.

Soluble cytokine receptors can be generated by different molecular mechanisms¹⁷. For the sIL-6R, alternative splicing of the IL-6R pre-mRNA, which results in the excision of the exon encoding the transmembrane region¹⁸, and proteolytic cleavage of the membrane-bound IL-6R have been described¹⁹. Different proteases have been implicated in sIL-6R generation, e.g. neutrophil-derived serine proteases²⁰ or meprins²¹. However, most work done to date has concentrated on the two metalloproteases ADAM10 and ADAM17. ADAM17 can be activated by different stimuli to provoke IL-6R cleavage, including the phorbol ester PMA^{19,22}, cellular cholesterol depletion²³ or apoptosis²⁴. ADAM10 cleaves the IL-6R constitutively, but can also be stimulated to do so, e.g. by the ionophore ionomycin or via activation of the purinergic P2X7 receptor^{25–27}. We have recently shown that the majority of about 85% of sIL-6R in the human circulation is generated via proteolysis, whereas the remaining ~ 15% are the result of alternative splicing²⁸. The C-terminus of the proteolysis-derived sIL-6R ends with Pro-355, which means that the protease that cleaves the IL-6R *in vivo* uses the cleavage site between Pro-355 and Val-356. We have further demonstrated that ADAM17 uses exactly this cleavage site *in vitro* and that mutation of Val-356 is sufficient to generate an IL-6R variant that is not cleaved by ADAM17²⁸. However, sIL-6R serum levels are unaltered in hypomorphic ADAM17^{ex/ex} mice, suggesting that another protease besides ADAM17 is responsible for the generation of sIL-6R serum levels under physiological conditions.

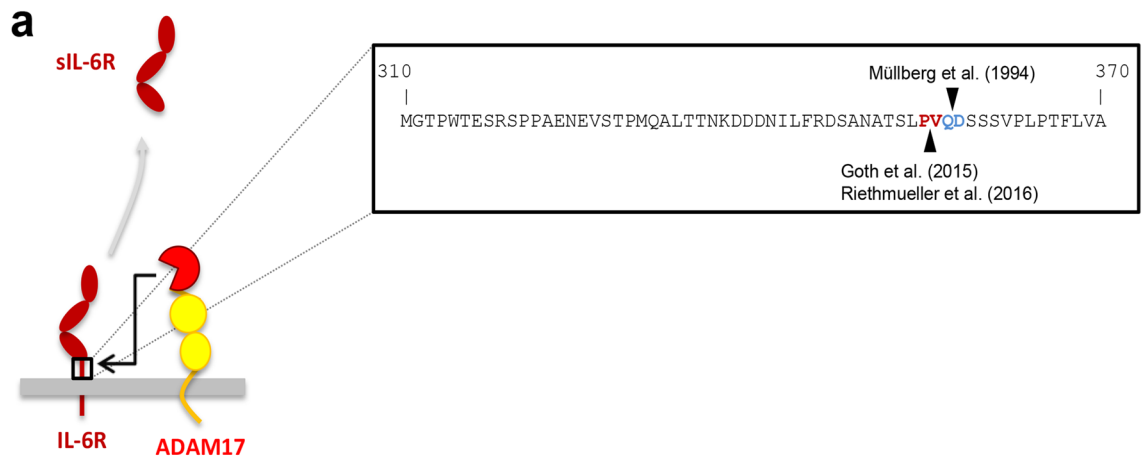
Cysteine cathepsins are a group of proteases with 11 members in humans²⁹. Traditionally viewed as important degrading enzymes present in lysosomes, it is becoming more and more evident that cysteine cathepsins have crucial additional roles that are not restricted to the lysosome. Some family members are also present in other cellular compartments and even secreted as active proteases into the extracellular space^{29,30}. One of the secreted family members is cathepsin S (CTSS), which is predominantly expressed in antigen-presenting cells³¹. Secreted CTSS is able to cleave membrane-bound substrates, e.g. the chemokine fractalkine³², which is due to the fact that CTSS, in contrast to most other cathepsins, is biologically activate at a neutral pH and thus does not require an acidic environment³³.

In this study, we identify CTSS as a novel protease that can cleave the IL-6R. The sIL-6R generated by CTSS is biologically active and able to induce IL-6 trans-signaling. However, CTSS does not use the same cleavage site as ADAM17 and does not contribute to the generation of sIL-6R steady state levels in mice.

Results

Identification of candidate proteases for IL-6R cleavage based on the cleavage site. The IL-6 trans-signaling pathway is initiated by cleavage of the membrane-bound IL-6R. Initial studies described a responsible protease that was activated by the phorbol ester PMA in a protein kinase C (PKC)-dependent manner¹⁹, which was later identified as ADAM17^{34,35}. The used cleavage site was originally identified to be located between Gln-357 and Asp-358 within the so-called stalk region of the IL-6R close to the plasma membrane (Fig. 1a and³⁶). Recent studies, however, could not reproduce this finding, but rather determined the ADAM17 cleavage site to be located between Pro-355 and Val-356 (Fig. 1a and^{28,37}). We determined the correct cleavage site of the IL-6R by ADAM17 via mass spectrometry (MS) analyses of precipitated sIL-6R from human serum and identified a C-terminal peptide of the sIL-6R that originated from proteolytic cleavage and ended with the residue Pro-355. We obtained the same result when we stimulated HEK293 cells overexpressing IL-6R with PMA and analyzed precipitated sIL-6R via MS. Furthermore, mutation of the Pro-355/Val-356 cleavage site abrogated ADAM17-mediated IL-6R cleavage. Thus, we conclude that the exact position of the ADAM17 cleavage site in the IL-6R is at Pro-355²⁸.

These results suggested that ADAM17 is the responsible protease that generates sIL-6R levels *in vivo*. However, the fact that the cleavage site, which ADAM17 uses *in vitro* is the same cleavage site that is used *in vivo* does not necessarily prove a causative role for ADAM17. Indeed, sIL-6R levels in hypomorphic ADAM17^{ex/ex} mice are unaltered compared to wild-type controls²⁵. Thus, we hypothesized that a different protease cleaves the IL-6R *in vivo* that simply uses the same IL-6R cleavage site as ADAM17 does *in vitro*. In order to identify candidate proteases, we searched the MEROPS database³⁸ for human proteases that are known to cleave their substrates between a proline and a valine residue. This search revealed 16 proteases (Fig. 1b), among them the known IL-6R sheddases ADAM17 and ADAM10²³. The other candidates are two cathepsins, 5 matrix metalloproteases (MMPs), one matrix-type MMP (MT-MMP) and the proteases neprilysin, carboxypeptidase A6, mast cell peptidase 5, dipeptidyl-peptidase IV, lysosomal Pro-Xaa carboxypeptidase and dipeptidyl-peptidase II (Fig. 1b). Importantly, this approach does neither take into consideration the cellular localization nor the cell-type specific expression of the proteases but is solely based on the cleavage site preferences. For example, dipeptidyl-peptidases II and IV, carboxypeptidase A6 and lysosomal Pro-Xaa carboxypeptidase are exopeptidases and therefore unable to release the ectodomain of transmembrane proteins, which excludes them as the sought-after IL-6R protease. Thus, it is expected that not all of the proteases are indeed IL-6R sheddases.



b

substrate	peptidase
HLA class II histocompatibility antigen gamma chain	cathepsin F
HLA class II histocompatibility antigen gamma chain	cathepsin S
20 annotated substrates	matrix metallopeptidase-2
SPARC	matrix metallopeptidase-9
20 annotated substrates	matrix metallopeptidase-3
Cadherin-1 precursor / plasminogen	matrix metallopeptidase-7
aggrecan core protein / SPARC	matrix metallopeptidase-13
HB-EGF / heparin-binding EGF-like growth factor precursor / protein-glutamine gamma-glutamyltransferase 2	membrane-type matrix metallopeptidase-1
p75NTR	ADAM10 peptidase
heparin-binding EGF-like growth factor precursor / tumor necrosis factor receptor superfamily member 16	ADAM17 peptidase
Corticotropin / melanotropin alpha	neprilysin
secretogranin-1	carboxypeptidase A6
Suc-Ala-Ala-Pro-Val-pNA	mast cell peptidase 5
C-X-C motif chemokine 9 / small inducible cytokine B6 / stromal cell-derived factor 1	dipeptidyl-peptidase IV (eukaryote)
Z-Pro-Val	lysosomal Pro-Xaa carboxypeptidase
His-Pro-Val	dipeptidyl-peptidase II

Figure 1. Identification of candidate proteases for IL-6R cleavage based on the cleavage site. **(a)** Schematic representation of sIL-6R generation via IL-6R proteolysis by ADAM17. The amino acids comprising the stalk region (from Met-310 to Ala-370) are depicted in one letter code in the inset on the right side. Previously described IL-6R cleavage sites attributed to ADAM17 are indicated. **(b)** Candidate proteases that could cleave the IL-6R between Pro-355 and Ala-356 based on the annotations found in the MEROPS database. For details see *Materials and Methods*.

Expression profile of cathepsin S. In order to validate whether our search approach based on the cleavage site (Fig. 1b) resulted at all in proteases that can cleave the IL-6R, we chose cathepsin S (CTSS) for further investigation. The reasons for investigating CTSS were that (1) the annotated substrate in the MEROPS database was a protein and not just a peptide (Fig. 1b) and (2) CTSS has been linked previously not only to inflammatory

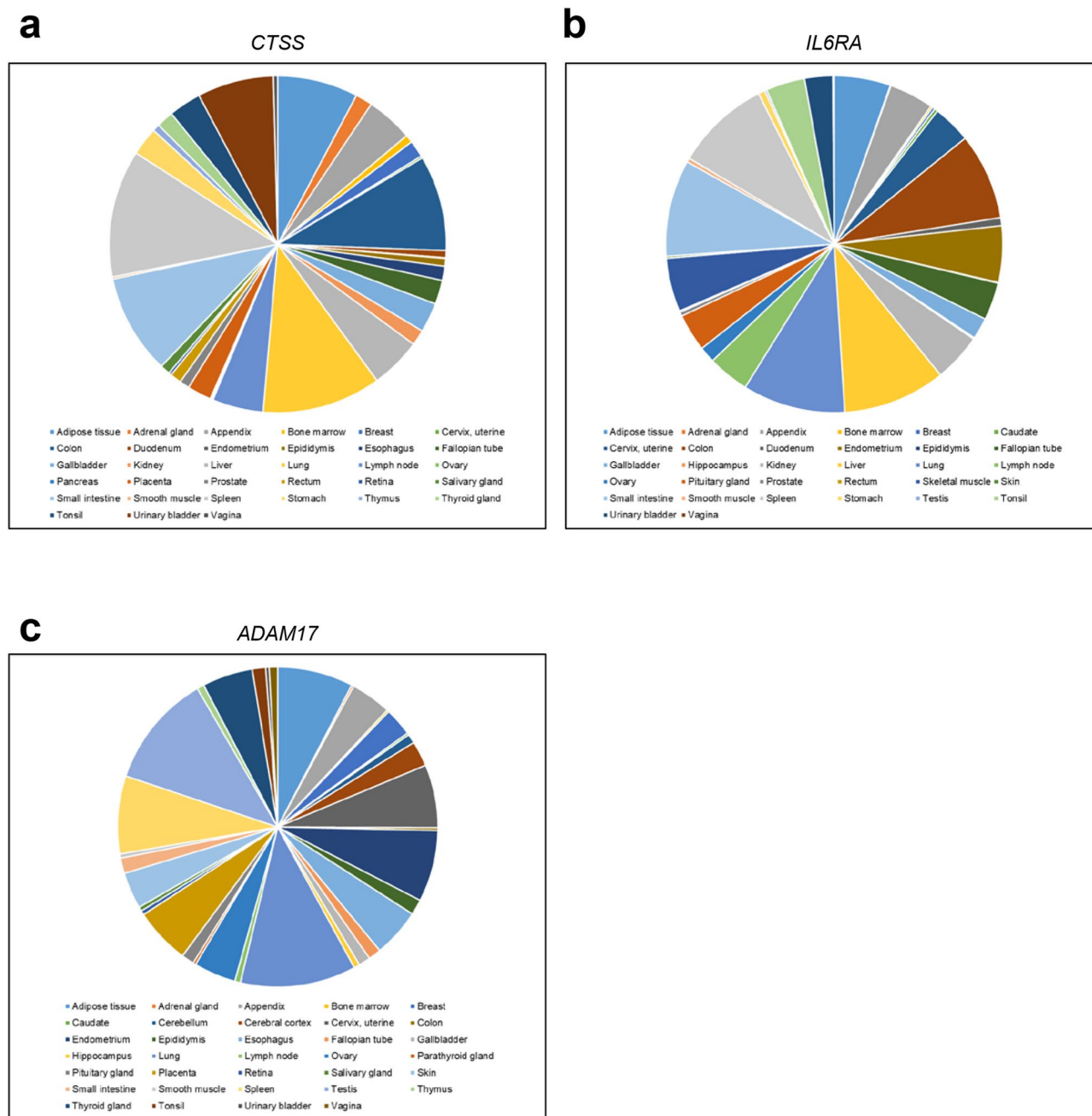


Figure 2. Expression profile of human *CTSS*, *IL6RA* and *ADAM17*. The pie charts show the twenty tissues with the highest expression of (a) *CTSS*, (b) *IL6RA* and (c) *ADAM17*. Expression data were analyzed as described previously⁴⁴.

processes^{39,40}, but also directly to IL-6^{41,42}. For an IL-6R protease, one would expect that it is expressed in similar cell types as the IL-6R. In order to determine this, we analyzed mRNA expression of *CTSS*, *IL-6R* and *ADAM17* in different human tissues. For this, we used quantitative expression data from the human protein atlas (v18, [proteinatlas.org](https://www.proteinatlas.org))⁴³ and a scoring system developed by Düsterhöft et al.⁴⁴ (Fig. 2a–c). Intriguingly, expression of *CTSS* and *IL-6R* highly correlated (Pearson Correlation 0.439, $p = 0.003$), and the same was true for *ADAM17* and *IL-6R* (Pearson Correlation 0.716, $p < 0.001$) (Table 1). Thus, the expression pattern of *CTSS* and *IL-6R* open up the possibility that *CTSS* might indeed be a protease that could cleave the *IL-6R*.

IL-6R peptide cleavage by cathepsin S and ADAM17. Despite an initial report that the recombinant catalytic domain of *ADAM17* is not capable of cleaving a peptide corresponding to a part of the *IL-6R* stalk region containing its cleavage site⁴⁵, we²⁸ and others³⁷ have reported recently that such peptides are indeed processed at the correct Pro/Val cleavage site. Importantly, however, the *IL-6R* peptide is still a rather bad substrate for recombinant *ADAM17*, especially compared to corresponding peptides of *TNF α* , even after long incubation

	CTSS	IL6RA	ADAM17
CTSS			
Pearson correlation	1.000		
Sig. (2-tailed)	–		
N	60		
IL6RA			
Pearson correlation	0.439**	1.00	
Sig. (2-tailed)	0.003	–	
N	45	60	
ADAM17			
Pearson correlation	0.512**	0.716**	1.00
Sig. (2-tailed)	0.001	0.000	–
N	39	39	60

Table 1. Matrix of correlations. **Correlation is significant at the 0.01 level (2-tailed).

times²⁸. We reasoned that recombinant CTSS should behave similarly and thus employed a peptide cleavage assay using three different internally quenched peptides containing the MCA/DNP pair, which emit fluorescence once the peptide is cleaved by a protease (Fig. 3a). The first peptide, named IL-6R_PVQD, consists of ten amino acid residues of the wild-type IL-6R with the Pro/Val cleavage site in its center. This peptide is cleaved slowly by recombinant ADAM17 (Fig. 3b), which is consistent with our previous data²⁸. Importantly, recombinant CTSS was also able to cleave the IL-6R_PVQD peptide (Fig. 3b). Next, we analyzed cleavage of the IL-6R_PVQA peptide. Here, the aspartic acid residue at position 8 (corresponding to position P3' of the cleavage site) was replaced with an alanine residue (Fig. 3a). This peptide corresponds to an IL-6R variant encoded by the single nucleotide polymorphism (SNP) rs2228145, which leads to the aforementioned exchange of Asp358Ala of the IL-6R and results in increased sIL-6R levels^{11,12} due to enhanced proteolytic cleavage^{10,28}. In line with this and compared to the IL-6R_PVQD peptide (Fig. 3b), the IL-6R_PVQA peptide was cleaved more rapidly by ADAM17 and CTSS as illustrated by an increase in fluorescence over time (Fig. 3c). As we have previously shown that mutation of the valine residue within the IL-6R cleavage site abrogated ADAM17-mediated cleavage²⁸, we used lastly the peptide IL-6R_PGQD, which showed indeed strongly reduced cleavage by both ADAM17 and CTSS (Fig. 3d). In summary, our peptide cleavage data not only show that CTSS can cleave a peptide containing the IL-6R cleavage site, but also that CTSS behaves remarkably similar to ADAM17 regarding this cleavage site.

Cathepsin S generates a biologically active sIL-6R independent of ADAM10 and ADAM17. In order to investigate whether CTSS would also be able to release sIL-6R from cells, we transfected HEK293 cells and therefore overexpressed IL-6R together with either CTSS or GFP. We exchanged the medium 24 h after transfection and harvested the conditioned medium after different periods of time (0–24 h). As shown in Fig. 4a, HEK293 cells transfected with IL-6R and GFP released sIL-6R over time as measured by ELISA, consistent with previous findings that ADAM10 constitutively cleaves IL-6R^{23,25,26}. This was three-fold increased when IL-6R and CTSS were both expressed in HEK293 cells, suggesting that CTSS was indeed able to perform IL-6R cleavage (Fig. 4a). Cells expressing either GFP alone or GFP in combination with CTSS served as control and did not release sIL-6R (Fig. 4a). To prove that the released sIL-6R resulted from direct cleavage by the expressed CTSS and was not indirectly released by one of the known IL-6R sheddases, we repeated the experiment using HEK293 cells deficient for ADAM10 and ADAM17 (HEK293-ADAM10^{-/-}/ADAM17^{-/-}), which we have described previously²⁷. We detected strongly reduced sIL-6R release when these cells were transfected with IL-6R and GFP compared to HEK293 wt, but unaltered sIL-6R release when IL-6R and CTSS were co-expressed (Fig. 4b). These results show that ADAM10 and ADAM17 are not involved in sIL-6R generation by CTSS and indicate a direct proteolysis of the IL-6R by CTSS.

In order to investigate whether the sIL-6R generated by overexpressed CTSS was biologically active, we made use of the pre-B cell line Ba/F3-gp130. These cells proliferate in the presence of IL-6/sIL-6R complexes and undergo apoptosis otherwise⁴⁶. Ba/F3-gp130 proliferated with supernatant containing sIL-6R cleaved by endogenous ADAM10 (IL-6R + DMSO), endogenous ADAM17 (IL-6R + PMA) and overexpressed CTSS (IL-6R + CTSS) when combined with recombinant IL-6 (Fig. 4c). This indicates that the sIL-6R generated by CTSS is indeed biologically active. However, IL-6R can also be released from cells on microvesicles⁴⁷, and it might be possible that CTSS expression does not directly lead to IL-6R cleavage, but rather to the stimulation of the release of microvesicles containing IL-6R. In order to exclude this possibility, we performed ultracentrifugation of the supernatants, which would remove microvesicles but keep sIL-6R derived from proteolysis. As shown in Fig. 4c, ultracentrifugation did not reduce proliferation of Ba/F3-gp130 cells, which is consistent with our findings that CTSS directly cleaves the IL-6R.

Cathepsin S uses a different IL-6R cleavage site than ADAM17. Having shown that CTSS is able to release a biologically active sIL-6R, we sought to investigate whether CTSS would indeed use the previously identified cleavage site between Pro-355 and Val-356. We again transiently transfected HEK293 with different combinations of expression plasmids encoding IL-6R, CTSS and GFP (Fig. 5a). When we precipitated proteins

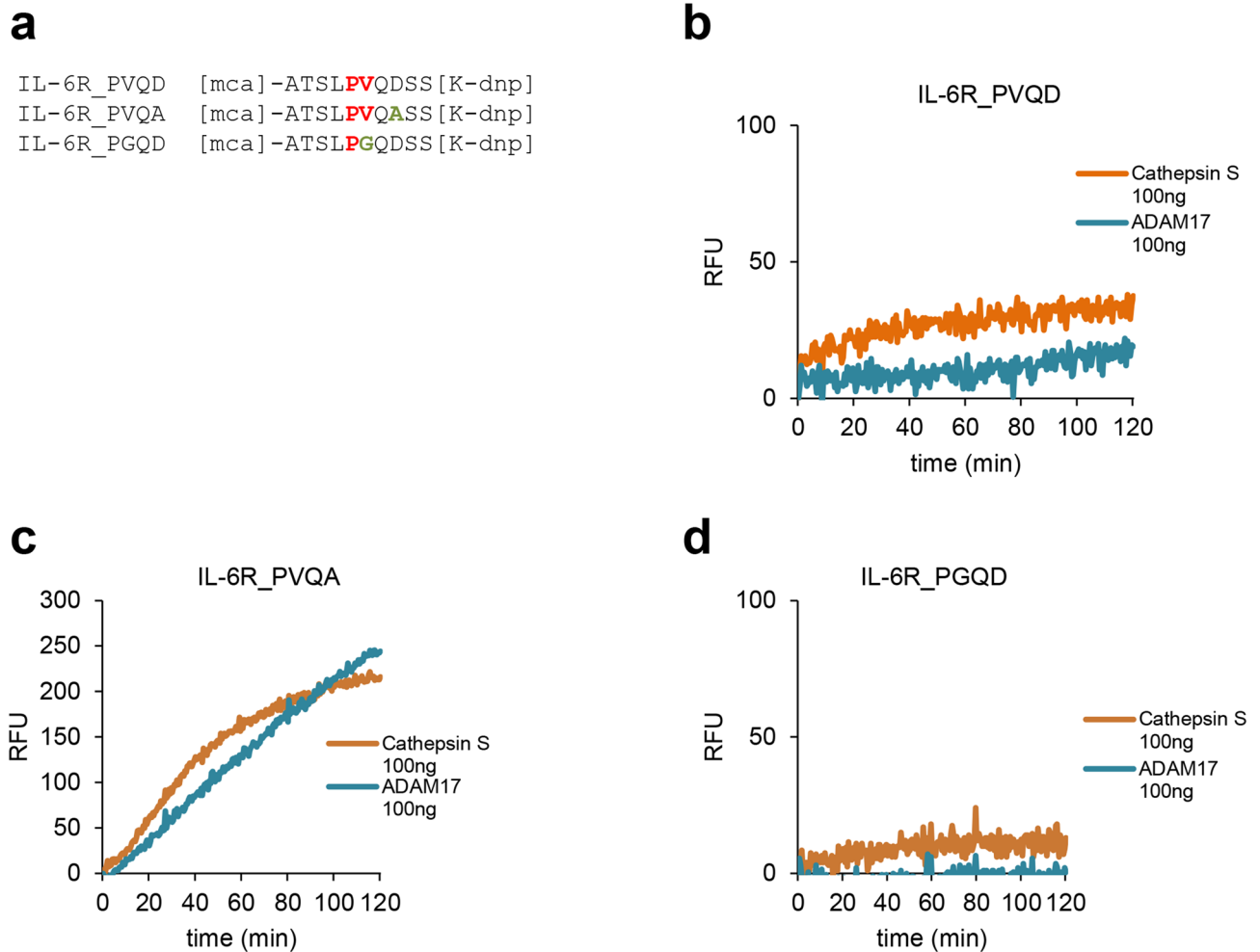


Figure 3. IL-6R peptide cleavage by Cathepsin S and ADAM17. **(a)** Sequences of the three peptides that were used in the experiments. IL-6R_PVQD corresponds to the wild-type sequence of the IL-6R, IL-6R-PVQA corresponds to an IL-6R containing the SNP rs2228145¹⁰ and IL-6R_PGQD corresponds to an IL-6R variants previously shown not to be cleaved by ADAM17²⁸. **(b–d)** Proteolysis of the three peptides by recombinant Cathepsin S (100 ng) and recombinant ADAM17 (100 ng) as measured via an increase in fluorescence over 120 min.

from the supernatant of cells overexpressing IL-6R and CTSS, we detected two bands of different molecular weights around 80 kDa and 55 kDa. We concluded that the smaller sIL-6R derived probably from proteolysis by CTSS, while the larger IL-6R could be the full length variant on microvesicles that we had described previously⁴⁷. Intriguingly, when we analyzed the supernatant of IL-6R-expressing HEK293 cells that had been stimulated with PMA to induce sIL-6R generation by ADAM17, the ADAM17-generated sIL-6R had a considerable higher molecular weight compared to the sIL-6R generated by CTSS (Fig. 5a). This suggests that overexpressed CTSS and endogenous ADAM17 do not use the same cleavage site when cleaving the full-length IL-6R protein. Importantly, we observed the same pattern of sIL-6R variants in the supernatant of HEK293-ADAM10^{-/-}/ADAM17^{-/-} cells, which further underlines that sIL-6R generation is mediated directly by CTSS and does not involve ADAM10 and ADAM17 (Fig. 5a).

We have previously described different IL-6R variants that carry deletions within the stalk region²⁶. In order to determine the region in which CTSS cleaves the IL-6R, we chose IL-6RΔS353_V362, IL-6RΔI343_T352 and IL-6RΔA333_N342, which lack consecutive stretches of 10 amino acid residues, and IL-6RΔS353_F367, which lacks the 15 amino acid residues adjacent to the plasma membrane (Fig. 5b). We transiently expressed IL-6R wild-type and the four IL-6R variants either together with GFP or with CTSS in HEK293 cells and analyzed sIL-6R generation by Western blot (Fig. 5c). For all IL-6R variants, we detected an IL-6R species in the supernatant with roughly the same molecular weight as the full-length construct found in the cell lysate (Fig. 5d). This sIL-6R was seen independent of CTSS co-expression and disappeared completely after ultracentrifugation of the supernatant, which is consistent with an IL-6R released on microvesicles. The smaller sIL-6R species only present when CTSS was co-expressed did not disappear after ultracentrifugation, indicative of soluble proteins derived from proteolysis (Fig. 5c). The cleavage product produced by overexpressed CTSS was clearly visible for all tested IL-6R variants with the exception of IL-6RΔI343_T352, for which only a faint band could be detected (Fig. 5c). In line

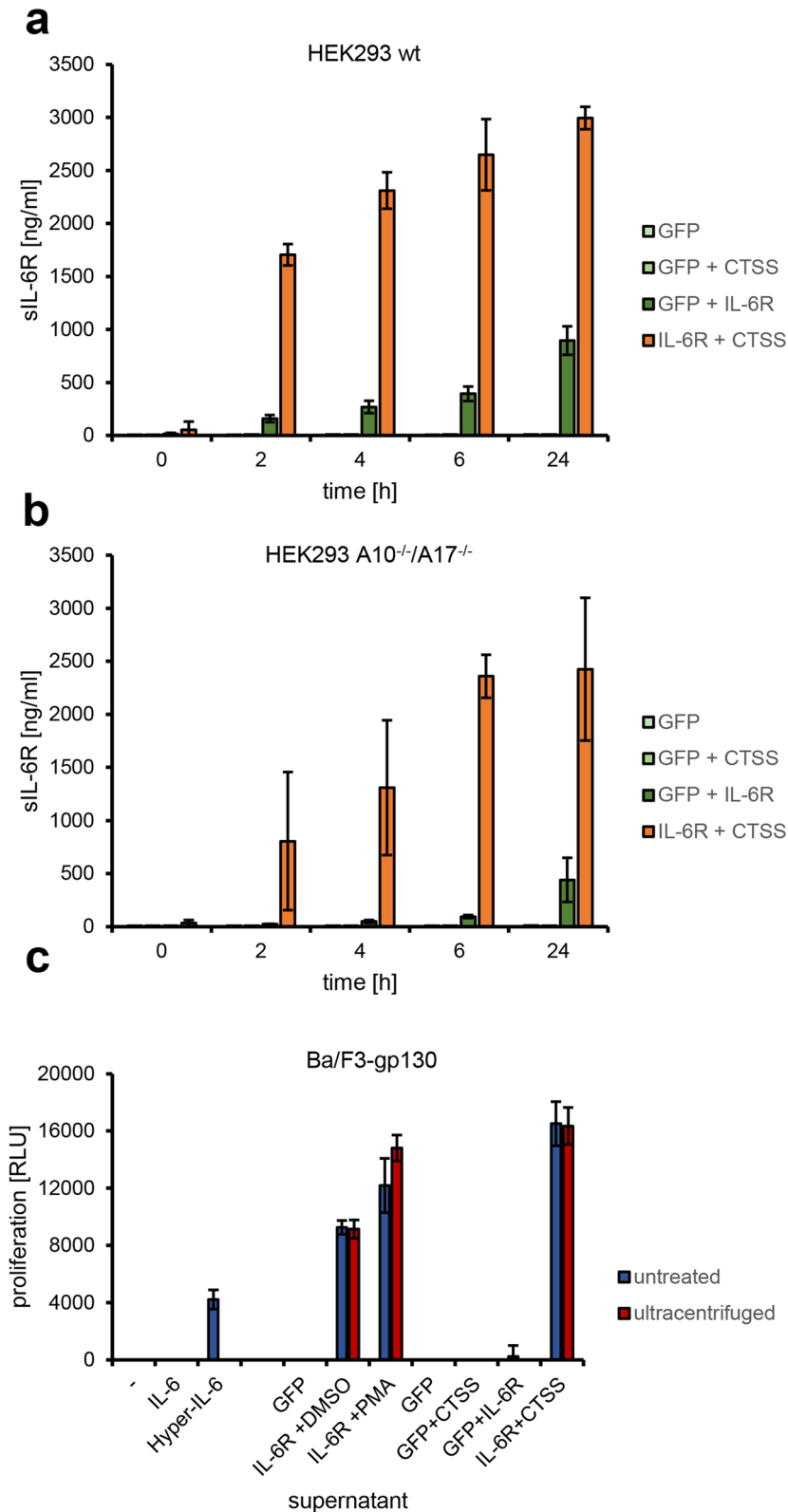
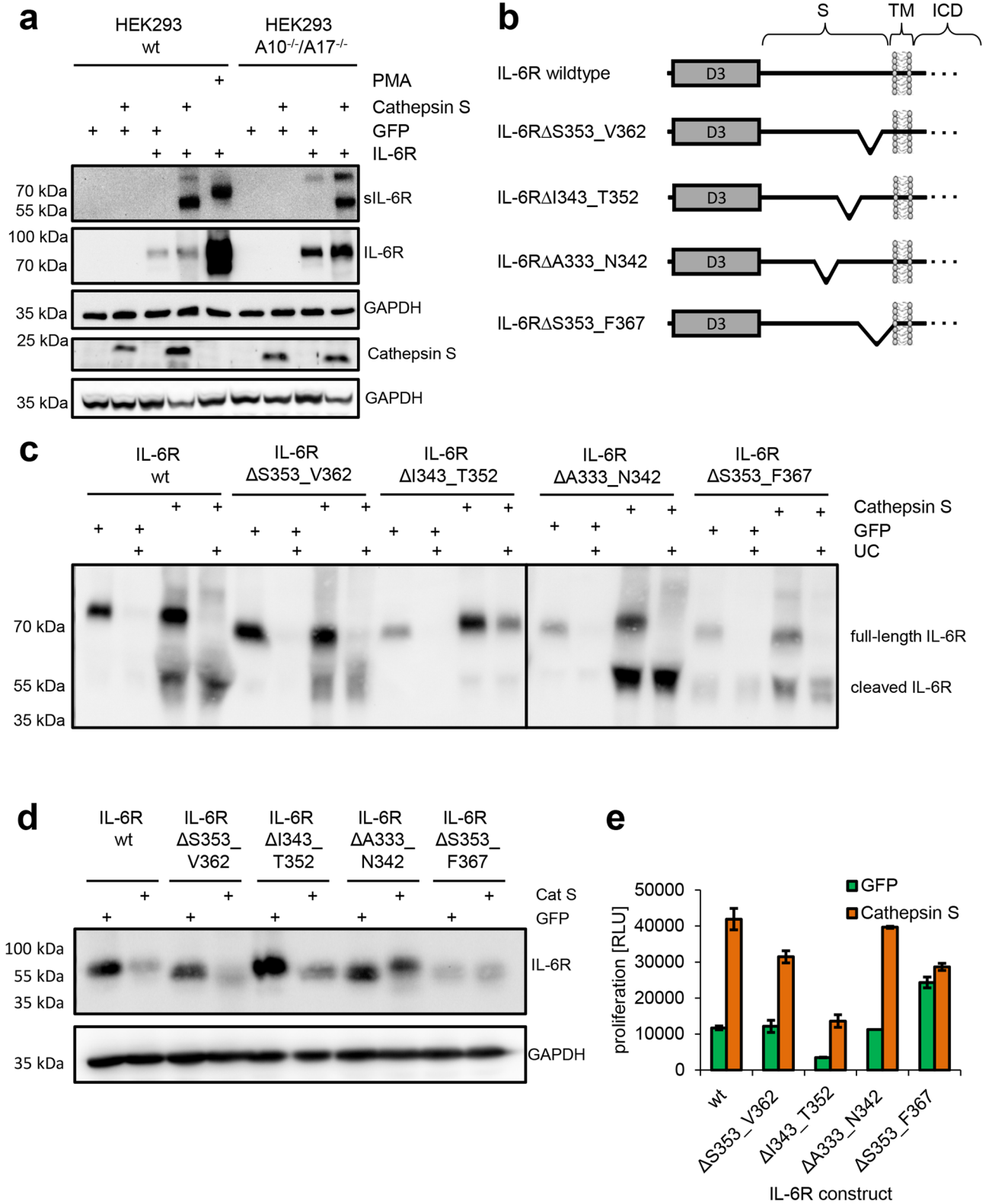


Figure 4. Cathepsin S generates a biologically active sIL-6R independent of ADAM10 and ADAM17. **(a)** HEK293 cells were transiently transfected with expression plasmids encoding GFP and CTSS, GFP and IL-6R, IL-6R and CTSS or only with an expression plasmid encoding GFP. The medium was exchanged 24 h after transfection and the conditioned medium harvested after different periods of time (0–24 h). The amount of sIL-6R in the medium was determined by ELISA (mean ± SD). **(b)** The experiment was performed as described for panel (a), but HEK293-ADAM10^{-/-}/ADAM17^{-/-} cells were used instead. **(c)** In order to investigate whether the sIL-6R generated by CTSS was biologically active, equal amounts of Ba/F3-gp130 cells were stimulated with recombinant proteins and/or supernatants as indicated. Cell proliferation as measured by cell viability was determined 48 h later. Red colored bars indicate supernatant after ultracentrifugation, whereas the blue bars indicate supernatant without ultracentrifugation.



◀ **Figure 5.** Cathepsin S uses a different IL-6R cleavage site than ADAM17. **(a)** The experiment was performed as described in the legends to panels Fig. 4a,b, but the sIL-6R was precipitated from the supernatant and visualized by western blotting. Furthermore, HEK293 cells transiently transfected with an expression plasmid encoding IL-6R were stimulated with PMA for 120 min, which activates ADAM17 and induces IL-6R proteolysis. The cells were lysed and also visualized by western blotting. GAPDH was determined to verify equal protein loading. Overexpressed Cathepsin S was visualized by Western blotting in an experiment that was conducted similarly, and GAPDH was determined to verify equal protein loading. **(b)** Schematic representation of the different IL-6R constructs that were used to map the cleavage site used by CTSS. The IL-6R constructs have been described previously²⁶. **(c)** HEK293 cells were transiently transfected with expression plasmids encoding IL-6R in combination with either GFP or CTSS. The experiment was performed as described in the legend of panel **(a)**, but before precipitation the supernatants were split in half and either ultracentrifuged or left untreated. **(d)** Western blot of the cell lysates corresponding to the supernatants shown in panel **(c)**. GAPDH was determined to verify equal protein loading. **(e)** The experiment was performed as described in the legend to Fig. 4c. Supernatants of HEK293 cells transiently transfected with expression plasmids encoding the different IL-6R variants depicted below the bar diagram in combination with either CTSS or GFP were used.

with this, conditioned supernatant derived from transfected HEK293 cells resulted in the weakest proliferation of Ba/F3-gp130 cells when supernatant from IL-6RAI343_T352 transfected cells was combined with recombinant IL-6 (Fig. 5e). We concluded from these experiments that CTSS and ADAM17 do not use the same cleavage site and that overexpressed CTSS instead uses a cleavage site further N-terminal between Ile-343 and Thr-352.

Cathepsin S does not contribute to constitutive sIL-6R generation in vivo. Serum levels of sIL-6R in humans are in the range of 20–80 ng/ml and in mice between 5 and 20 ng/ml. We have previously shown that in humans, the majority of sIL-6R is generated by proteolysis²⁸ and that serum levels in ADAM17^{ex/ex} mice are unchanged compared to wild-type animals²⁵. To determine whether CTSS contributes to sIL-6R levels in mice, we analyzed serum samples of *Ctss*^{-/-} mice. Compared to wild-type controls, we found no difference in sIL-6R serum levels (Fig. 6), which excludes a major role of CTSS in the generation of the steady state sIL-6R levels in mice.

Discussion

The cytokine IL-6 is an important therapeutic target in inflammatory diseases, but possesses a very complex biology, which makes the development of therapeutic compounds without unwanted adverse effects challenging³. This is mostly due to the fact that IL-6 can signal via membrane-bound and soluble variants of the IL-6R and that the so-called trans-signaling of IL-6 is responsible for the pro-inflammatory functions of the cytokine. Therefore, a selective inhibition of signaling via the sIL-6R, which would leave classic signaling via the membrane-bound IL-6R untouched and preserve e.g. the hepatic acute phase response, holds the promise to be a next-generation therapeutic with a superior safety profile compared to the total blockade of IL-6 activity achieved with anti-IL-6 or anti-IL-6R antibodies that are already in clinical use³.

Several inflammatory stimuli are known that lead to the cleavage of the IL-6R at the plasma membrane and an increase in local sIL-6R levels, thus fostering IL-6 trans-signaling. These include apoptosis²⁴, listeria monocytogenes infection⁴⁸ or the activation of Toll-like receptor 2⁴⁹ or the T cell receptor⁵⁰. In all these contexts, the protease that cleaves the IL-6R upon stimulation has been identified as ADAM17, using specific chemical inhibitors and genetically modified mice, which makes it easy to assume that ADAM17-mediated IL-6R proteolysis represents a major mechanism for sIL-6R generation under inflammatory conditions.

However, how the steady state sIL-6R serum levels, which are present in mice and humans under normal physiological conditions, are generated is less well understood. We have shown previously that alternative mRNA splicing accounts for ~15% and that proteolytic cleavage accounts for ~85% of the sIL-6R found in human serum²⁸. We were able to map the used cleavage site precisely via MS analyses, which is located in close proximity to the plasma membrane within the so-called stalk region of the IL-6R between Pro-355 and Val-356. Intriguingly, ADAM17 uses exactly the same cleavage site in vitro, making it a likely candidate for producing also the steady state sIL-6R serum levels²⁸. However, hypomorphic ADAM17^{ex/ex} mice, in which the serum levels of other ADAM17 substrates are significantly reduced⁵¹, show unaltered sIL-6R levels, which implies that either ADAM17 is not the responsible protease, or that in the absence of ADAM17, another protease takes over the cleavage of the IL-6R.

We have therefore attempted to identify further candidate proteases that might be involved in sIL-6R generation. Based on the known cleavage site, we have mined the MEROPS database and found several proteases that could potentially cleave the IL-6R. We have concentrated on cathepsin S (CTSS), because its cellular expression profile matches the one of the IL-6R, it can be secreted from cells and would therefore be able to access the IL-6R, and finally because it is known to be involved in inflammatory reactions^{39,40}. CTSS behaved in our initial peptide cleavage assays like ADAM17 and was able to release a biologically active sIL-6R in cellular assays that could bind IL-6 and perform trans-signaling on cells that lack the membrane-bound IL-6R and would thus without the sIL-6R not react to IL-6 alone. However, two important findings made it unlikely that CTSS was the protease we searched for. Using different IL-6R stalk mutants, we could show that CTSS does not use the cleavage site between Pro-355 and Val-356 that we had determined previously, but rather cleaves the IL-6R at a position further N-terminal within the stalk region, which excludes that CTSS is involved in sIL-6R generation in humans. Secondly, the serum levels in healthy *Ctss*^{-/-} mice were unaltered compared to wild-type control mice, judging against an involvement of this protease in sIL-6R generation also in mice.

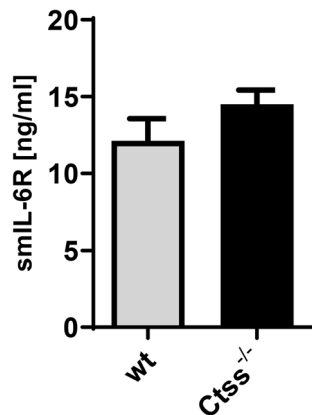


Figure 6. Cathepsin S does not contribute to constitutive sIL-6R generation in vivo. Levels of sIL-6R were determined via ELISA in serum samples from three wild-type and three *Ctss*^{-/-} mice (mean ± SD).

In conclusion, although we were able to identify a novel protease that can cleave the IL-6R and thus activate IL-6 trans-signaling, which might be important for example under inflammatory conditions in which CTSS is overexpressed, our data rule out a contribution of CTSS to the formation of the steady-state sIL-6R serum levels. Further research is needed to identify the responsible protease(s) for this.

Methods

Cells and reagents. HEK293 and HEK293-ADAM10^{-/-}/ADAM17^{-/-} cells, which have been described previously²⁷, were cultured in DMEM high-glucose culture medium (Gibco/Thermo Fisher Scientific, Waltham, MA, USA) supplemented with 10% fetal bovine serum, penicillin (60 mg/l), and streptomycin (100 mg/l). All cells were kept at 37 °C and 5% CO₂ in a standard incubator with a water-saturated atmosphere. Cells were transiently transfected with the cationic polymer solution TurboFect Transfection Reagent (Thermo Fisher Scientific, Waltham, MA, USA). Expression plasmids encoding IL-6R and Cathepsin S have been described previously^{25,52}. The protein kinase C activator phorbol-12-myristate-13-acetate (PMA) was purchased from Sigma-Aldrich (St. Louis, MO, USA). The peptides [mca]-ATSLPVQDSS[K-dnp] (IL-6R_PVQD), [mca]-ATSLPVQASS[K-dnp] (IL-6R_PVQA) and [mca]-ATSLPGQDSS[K-dnp] (IL-6R_PGQD) were synthesized by Genosphere Biotechnologies (Paris, France). The cytokine IL-6 was expressed and purified as described previously⁵³, as well as the designer cytokine Hyper-IL-6^{46,54}. The antibody 4–11 (IL-6R antibody) was also expressed and purified as described previously²⁴. The GAPDH antibody was purchased from Cell Signaling Technology (Frankfurt/M., Germany), the polyclonal rabbit anti-human Cathepsin S antibody (LS-C348945) was from LSBio (Seattle, WA, USA), and the secondary antibodies mouse-HRP and rabbit-HRP were obtained from Dianova (Hamburg, Germany). The recombinant protease cathepsin S was purchased from R&D systems (Minneapolis, USA).

Ectodomain shedding assay. HEK293 wt and HEK293-ADAM10^{-/-}/ADAM17^{-/-} cells were transiently transfected with plasmids coding for GFP, CTSS and different IL-6R variants. Two days after the transfection, the medium was exchanged with 5 ml fresh serum-free DMEM and the cells were incubated for 24 h at 37 °C before supernatants and cells were collected. Cells were lysed and supernatants were either used directly for protein precipitation by 20% TCA or were ultra-centrifuged (60 min at 4 °C and 100,000 g) before use. Finally, precipitated supernatants and lysates were analyzed by semi-dry western immunoblotting, which was performed as described previously²⁸.

Ba/F3-gp130 cell viability assay. To analyze whether generated sIL-6R is biologically active, a cell viability assay was performed using Ba/F3-gp130 cells and the CellTiter Blue Viability Assay (Promega, Karlsruhe, Germany) following the manufacturer's instructions. Ba/F3-gp130 cells were washed with PBS, resuspended in DMEM supplemented with 10% FCS and 1% PenStrep solution and 5000 cells in 50 µl cell culture medium were transferred in wells of a 96-well plate. 50 µl of conditioned medium from transfected HEK293 cells or, as control, fresh medium was added to the cells. The cells were incubated with IL-6 (25 ng/ml), Hyper-IL-6 (10 ng/ml) or without cytokine for 48 h at 37° and 5% CO₂ before 20 µl Cell Titer Blue Viability Assay reagent was added. Fluorescence intensity (RLU; relative light units) was measured at λ_{em} = 590 nm using the Synergy HTX multi-mode reader (BioTek, Winooski, VT, USA). Fluorescence at time point 60 min was normalized by subtracting the fluorescence measured at time point 0 min.

Quantification of human and murine sIL-6R. For the detection of murine sIL-6R in murine sera the Mouse IL-6R alpha DuoSet ELISA (R&D systems, Minneapolis, USA) was performed according to the user instructions by addition of 1:10 diluted sera. Levels of human sIL-6R in cell culture supernatant was analyzed using the DuoSet Human IL-6Rα ELISA kit (R&D systems, Minneapolis, USA) following the user instructions with slight adaptations. ELISA plates were coated with 50 µl capture antibody overnight, washed, and 50 µl of undiluted cell culture supernatant was added. Following, the samples were incubated with 50 µl of detection

antibody before the enzymatic reaction was started using streptavidin–horseradish peroxidase and the peroxidase substrate BM blue POD (Roche, Mannheim, Germany). The reaction was stopped using 1.8 M sulfuric acid and the absorbance was read at 450 nm on a Tecan Spectra Rainbow plate reader (Tecan, Crailsheim, Germany).

All experiments were performed in accordance with relevant guidelines and regulations and approved by the responsible committee in Erlangen (Amt für Veterinärwesen und Gesundheitlichen Verbraucherschutz, approval #TS-6/12).

Peptide cleavage assay. For the peptide cleavage assay, 10 μ M of the three different quenched fluorogenic IL-6R peptides [mca]-ATSLPVQDSS[K-dnp], [mca]-ATSLPVQASS[K-dnp] or [mca]-ATSLPGQDSS[K-dnp] (synthesized by Genosphere Biotechnologies, Paris, France) were incubated with 100 ng of the proteases ADAM17 or Cathepsin S in a total volume of 100 μ l in PBS. Fluorescence was measured at λ_{em} = 405 nm and λ_{ex} = 320 nm at 37 °C with a spectrophotometer (Tecan) every 30 s for 120 min. The increase in relative fluorescence units (RFUs) after 120 min was normalized to fluorescence at 0 s.

In silico analyses. Candidate proteases were identified with the use of the MEROPS database (<https://www.ebi.ac.uk/merops/>)³⁸. Here, the function “Search by specificity” was used to search for proteases that are known to cleave substrates with a proline residue at the P1 and a valine residue at the P1' position. All non-human proteases were removed from the search results. The expression profiles shown in Fig. 2 were generated using an approach described previously⁴⁴.

Statistical analyses. Statistical analyses were performed with the Statistical Package for the Social Sciences (IBM SPSS Statistics for Windows, Version 25.0. Armonk, NY, USA). Pearson product-moment correlation coefficients were used to detect linear correlations between *CTSS*, *IL6RA*, and *ADAM17*. A high positive/negative correlation, ranging from -1 to $+1$, implies that high values of one measure correspond to high (positive correlation) or low (negative correlation) values of the other measure.

Data presentation. Unless stated otherwise, data are presented as mean \pm SD from at least three independent experiments. For western blots and Ba/F3-gp130 cell viability data, one experiment from at least three with similar outcome is shown.

Data availability

No restrictions on the availability of materials or information apply. Requests for data and material should be addressed to the corresponding author (christoph.garbers@med.ovgu.de).

Received: 15 July 2020; Accepted: 18 November 2020

Published online: 10 December 2020

References

- Garbers, C. *et al.* Plasticity and cross-talk of Interleukin 6-type cytokines. *Cytokine Growth Factor Rev.* **23**, 85–97 (2012).
- Waage, A., Brandtzaeg, P., Halstensen, A., Kierulf, P. & Espevik, T. The complex pattern of cytokines in serum from patients with meningococcal septic shock. Association between interleukin 6, interleukin 1, and fatal outcome. *J. Exp. Med.* **169**, 333–338 (1989).
- Garbers, C., Heink, S., Korn, T. & Rose-John, S. Interleukin-6: designing specific therapeutics for a complex cytokine. *Nat. Rev. Drug Discov.* **17**, 395–412 (2018).
- Jones, S. A. & Jenkins, B. J. Recent insights into targeting the IL-6 cytokine family in inflammatory diseases and cancer. *Nat. Rev. Immunol.* **18**, 773–789 (2018).
- Wolf, J., Rose-John, S. & Garbers, C. Interleukin-6 and its receptors: a highly regulated and dynamic system. *Cytokine* **70**, 11–20 (2014).
- Eulenfeld, R. *et al.* Interleukin-6 signalling: more than Jaks and STATs. *Eur. J. Cell Biol.* **91**, 486–495 (2012).
- Scheller, J., Garbers, C. & Rose-John, S. Interleukin-6: from basic biology to selective blockade of pro-inflammatory activities. *Semin. Immunol.* **26**, 2–12 (2014).
- Garbers, C., Aparicio-Siegmund, S. & Rose-John, S. The IL-6/gp130/STAT3 signaling axis: recent advances towards specific inhibition. *Curr. Opin. Immunol.* **34**, 75–82 (2015).
- Chalaris, A., Garbers, C., Rabe, B., Rose-John, S. & Scheller, J. The soluble Interleukin 6 receptor: generation and role in inflammation and cancer. *Eur. J. Cell Biol.* **90**, 484–494 (2011).
- Garbers, C. *et al.* The interleukin-6 receptor Asp358Ala single nucleotide polymorphism rs2228145 confers increased proteolytic conversion rates by ADAM proteases. *Biochim. Biophys. Acta* **1842**, 1485–1494 (2014).
- Rafiq, S. *et al.* A common variant of the interleukin 6 receptor (IL-6r) gene increases IL-6r and IL-6 levels, without other inflammatory effects. *Genes Immun.* **8**, 552–559 (2007).
- Galicía, J. *et al.* Polymorphisms in the IL-6 receptor (IL-6R) gene: strong evidence that serum levels of soluble IL-6R are genetically influenced. *Genes Immun.* **5**, 513–516 (2004).
- Sarwar, N. *et al.* Interleukin-6 receptor pathways in coronary heart disease: a collaborative meta-analysis of 82 studies. *Lancet* **379**, 1205–1213 (2012).
- Swerdlow, D. *et al.* The interleukin-6 receptor as a target for prevention of coronary heart disease: a mendelian randomisation analysis. *Lancet* **379**, 1214–1224 (2012).
- Scheller, J. & Rose-John, S. The interleukin 6 pathway and atherosclerosis. *Lancet* **380**, 338 (2012).
- Aparicio-Siegmund, S. *et al.* The IL-6-neutralizing sIL-6R-sgp130 buffer system is disturbed in patients with type 2 diabetes. *Am. J. Physiol. Endocrinol. Metab.* **317**, E411–E420 (2019).
- Lokau, J. & Garbers, C. Biological functions and therapeutic opportunities of soluble cytokine receptors. *Cytokine Growth Factor Rev.* **55**, 94–108 (2020).
- Lüst, J. *et al.* Isolation of an mRNA encoding a soluble form of the human interleukin-6 receptor. *Cytokine* **4**, 96–100 (1992).
- Müllberg, J. *et al.* The soluble interleukin-6 receptor is generated by shedding. *Eur. J. Immunol.* **23**, 473–480 (1993).

20. Bank, U. *et al.* Selective proteolytic cleavage of IL-2 receptor and IL-6 receptor ligand binding chains by neutrophil-derived serine proteases at foci of inflammation. *J. Interferon Cytokine Res.* **19**, 1277–1287 (1999).
21. Arnold, P. *et al.* Meprin metalloproteases generate biologically active soluble interleukin-6 receptor to induce trans-signaling. *Sci. Rep.* **7**, 44053 (2017).
22. Müllberg, J., Schooltink, H., Stoyan, T., Heinrich, P. & Rose-John, S. Protein kinase C activity is rate limiting for shedding of the interleukin-6 receptor. *Biochem. Biophys. Res. Commun.* **189**, 794–800 (1992).
23. Matthews, V. *et al.* Cellular cholesterol depletion triggers shedding of the human interleukin-6 receptor by ADAM10 and ADAM17 (TACE). *J. Biol. Chem.* **278**, 38829–38839 (2003).
24. Chalaris, A. *et al.* Apoptosis is a natural stimulus of IL6R shedding and contributes to the pro-inflammatory trans-signaling function of neutrophils. *Blood* **110**, 1748–1755 (2007).
25. Garbers, C. *et al.* Species specificity of ADAM10 and ADAM17 proteins in interleukin-6 (IL-6) trans-signaling and novel role of ADAM10 in inducible IL-6 receptor shedding. *J. Biol. Chem.* **286**, 14804–14811 (2011).
26. Baran, P., Nitz, R., Grötzing, J., Scheller, J. & Garbers, C. Minimal interleukin (IL)-6 receptor stalk composition for IL-6R shedding and IL-6 classic signaling. *J. Biol. Chem.* **288**, 14756–14768 (2013).
27. Riethmueller, S. *et al.* Cleavage site localization differentially controls interleukin-6 receptor proteolysis by ADAM10 and ADAM17. *Sci. Rep.* **6**, 25550 (2016).
28. Riethmueller, S. *et al.* Proteolytic origin of the soluble human IL-6R in vivo and a decisive role of N-glycosylation. *PLoS Biol.* **15**, e2000080 (2017).
29. Vidak, E., Javorsek, U., Vizovisek, M. & Turk, B. Cysteine cathepsins and their extracellular roles: shaping the microenvironment. *Cells* **8**, 264 (2019).
30. Olson, O. C. & Joyce, J. A. Cysteine cathepsin proteases: regulators of cancer progression and therapeutic response. *Nat. Rev. Cancer* **15**, 712–729 (2015).
31. Hsing, L. C. & Rudensky, A. Y. The lysosomal cysteine proteases in MHC class II antigen presentation. *Immunol. Rev.* **207**, 229–241 (2005).
32. Fonovic, U. P., Jevnikar, Z. & Kos, J. Cathepsin S generates soluble CX3CL1 (fractalkine) in vascular smooth muscle cells. *Biol. Chem.* **394**, 1349–1352 (2013).
33. Kirschke, H., Wiederanders, B., Bromme, D. & Rinne, A. Cathepsin S from bovine spleen. Purification, distribution, intracellular localization and action on proteins. *Biochem. J.* **264**, 467–473 (1989).
34. Moss, M. *et al.* Cloning of a disintegrin metalloproteinase that processes precursor tumour-necrosis factor- α . *Nature* **385**, 733–739 (1997).
35. Black, R. *et al.* A metalloproteinase disintegrin that releases tumour-necrosis factor- α from cells. *Nature* **385**, 729–762 (1997).
36. Müllberg, J. *et al.* The soluble human IL-6 receptor. Mutational characterization of the proteolytic cleavage site. *J. Immunol.* **152**, 4958–4968 (1994).
37. Goth, C. K. *et al.* A systematic study of modulation of ADAM-mediated ectodomain shedding by site-specific O-glycosylation. *Proc. Natl. Acad. Sci. USA* **112**, 14623–14628 (2015).
38. Rawlings, N. D., Waller, M. & Barrett, A. J. MEROPS: the database of proteolytic enzymes, their substrates and inhibitors. *Nucleic Acids Res.* **42**, D503–509 (2013).
39. Thanei, S. *et al.* Cathepsin S inhibition suppresses autoimmune-triggered inflammatory responses in macrophages. *Biochem. Pharmacol.* **146**, 151–164 (2017).
40. Memmert, S. *et al.* Role of cathepsin S in periodontal inflammation and infection. *Mediators Inflamm.* **2017**, 4786170 (2017).
41. Dekita, M. *et al.* Cathepsin S is involved in Th17 differentiation through the upregulation of IL-6 by activating PAR-2 after systemic exposure to lipopolysaccharide from *Porphyromonas gingivalis*. *Front. Pharmacol.* **8**, 470 (2017).
42. Kitamura, H. *et al.* IL-6-STAT3 controls intracellular MHC class II alpha beta dimer level through cathepsin S activity in dendritic cells. *Immunity* **23**, 491–502 (2005).
43. Uhlen, M. *et al.* Proteomics tissue-based map of the human proteome. *Science* **347**, 1260419 (2015).
44. Düsterhöft, S., Babendreyer, A., Giese, A. A., Flasshove, C. & Ludwig, A. Status update on iRhom and ADAM17: it's still complicated. *Biochim. Biophys. Acta Mol. Cell Res.* **1866**, 1567–1583 (2019).
45. Mohan, M. J. *et al.* The tumor necrosis factor- α converting enzyme (TACE): a unique metalloproteinase with highly defined substrate selectivity. *Biochemistry* **41**, 9462–9469 (2002).
46. Fischer, M. *et al.* A bioactive designer cytokine for human hematopoietic progenitor cell expansion. *Nat. Biotechnol.* **15**, 142–145 (1997).
47. Schumacher, N. *et al.* Shedding of endogenous interleukin-6 receptor (IL-6R) is governed by a disintegrin and metalloproteinase (ADAM) proteases while a full-length IL-6R isoform localizes to circulating microvesicles. *J. Biol. Chem.* **290**, 26059–26071 (2015).
48. Yan, I. *et al.* ADAM17 controls IL-6 signaling by cleavage of the murine IL-6Ra from the cell surface of leukocytes during inflammatory responses. *J. Leukoc. Biol.* **99**, 749–760 (2015).
49. Flynn, C. M. *et al.* Activation of toll-like receptor 2 (TLR2) induces interleukin-6 trans-signaling. *Sci. Rep.* **9**, 7306 (2019).
50. Briso, E., Dienz, O. & Rincon, M. Cutting edge: soluble IL-6R is produced by IL-6R ectodomain shedding in activated CD4 T cells. *J. Immunol.* **180**, 7102–7106 (2008).
51. Chalaris, A. *et al.* Critical role of the disintegrin metalloprotease ADAM17 for intestinal inflammation and regeneration in mice. *J. Exp. Med.* **207**, 1617–1624 (2010).
52. Hüttel, S. *et al.* Substrate determinants of signal peptide peptidase-like 2a (SPPL2a)-mediated intramembrane proteolysis of the invariant chain CD74. *Biochem. J.* **473**, 1405–1422 (2016).
53. van Dam, M. *et al.* Structure-function analysis of interleukin-6 utilizing human/murine chimeric molecules. Involvement of two separate domains in receptor binding. *J. Biol. Chem.* **268**, 15285–15290 (1993).
54. Schroers, A. *et al.* Dynamics of the gp130 cytokine complex: a model for assembly on the cellular membrane. *Protein Sci.* **14**, 783–790 (2005).

Acknowledgements

The authors thank Alyn Gerneth and Christian Bretscher for excellent technical assistance. This work was funded by grants from the Deutsche Forschungsgemeinschaft, Bonn, Germany (CRC877 Projects A9 to CB-P, A10 to CG, A14 to CG and SR-J and B7 to BS; CRC1181 Project A7 to DD), by the Bundesministerium für Bildung und Forschung (BMBF Grant “InTraSig”, Project B), and by the Cluster of Excellence ‘Inflammation at Interfaces’.

Author contributions

C.F. performed the experiments, analyzed the results and contributed to writing of the manuscript. Y.G. performed the statistical analyses. J.L. and R.W. provided experimental techniques. S.D. contributed to the tissue expression analysis. C.H.K.L., D.D., C.B.-P., B.S. and S.R.-J. provided critical reagents. C.G. analyzed the data

and wrote the manuscript. S.A.S. contributed to writing of the manuscript and supervised the study together with C.G. All authors reviewed the manuscript.

Funding

Open Access funding enabled and organized by Projekt DEAL.

Competing interests

The authors declare no competing interest.

Additional information

Supplementary information is available for this paper at <https://doi.org/10.1038/s41598-020-77884-4>.

Correspondence and requests for materials should be addressed to C.G.

Reprints and permissions information is available at www.nature.com/reprints.

Publisher's note Springer Nature remains neutral with regard to jurisdictional claims in published maps and institutional affiliations.



Open Access This article is licensed under a Creative Commons Attribution 4.0 International License, which permits use, sharing, adaptation, distribution and reproduction in any medium or format, as long as you give appropriate credit to the original author(s) and the source, provide a link to the Creative Commons licence, and indicate if changes were made. The images or other third party material in this article are included in the article's Creative Commons licence, unless indicated otherwise in a credit line to the material. If material is not included in the article's Creative Commons licence and your intended use is not permitted by statutory regulation or exceeds the permitted use, you will need to obtain permission directly from the copyright holder. To view a copy of this licence, visit <http://creativecommons.org/licenses/by/4.0/>.

© The Author(s) 2020